HHS Public Access

Author manuscript

Magn Reson Imaging. Author manuscript; available in PMC 2022 May 01.

Published in final edited form as:

Magn Reson Imaging. 2021 May ; 78: 42–51. doi:10.1016/j.mri.2021.02.004.

Relationships between spinal cord blood flow measured with flow alternating arterial spin labeling (FAIR) and neurobehavioral outcomes in rat spinal cord injury

Seongtaek Lee[1,2,*], **Natasha Wilkins**[2], **Brian D. Schmit**[1], **Shekar N. Kurpad**[2,3], **Matthew D. Budde**[2,3]

[1]Department of Biomedical Engineering, Marquette University & Medical College of Wisconsin, Milwaukee, WI,

[2]Department of Neurosurgery, Medical College of Wisconsin, Milwaukee, WI,

[3]Clement J. Zablocki Veterans Affairs Medical Center, Milwaukee, WI

Abstract

In the traumatically injured spinal cord, decreased perfusion is believed to contribute to secondary tissue damage beyond the primary mechanical impact, and restoration of perfusion is believed to be a promising therapeutic target. However, methods to monitor spinal cord perfusion non-invasively are limited. Perfusion magnetic resonance imaging (MRI) techniques established for the brain have not been routinely adopted to the spinal cord. The purpose of this study was to examine the relationship between spinal cord blood flow (SCBF) and injury severity in a rat thoracic spinal cord contusion injury (SCI) model using flow-alternating sensitive inversion recovery (FAIR) with two variants of the label position. SCBF as a marker of severity was compared to T_1 mapping and to spinal cordoptimized diffusion weighted imaging (DWI) with filtered parallel apparent diffusion coefficient. Thirty-eight rats underwent a T10 contusion injury with varying severities (8 sham; 10 mild; 10 moderate; 10 severe) with MRI performed at 1 day post injury at the lesion site and follow-up neurological assessments using the Basso, Beattie, Bresnahan (BBB) locomotor scoring up to 28 days post injury. Using whole-cord regions of interest at the lesion epicenter, SCBF was decreased with injury severity and had a significant correlation with BBB scores at 28 days post injury. Importantly, estimates of arterial transit times (ATT) in the injured spinal cord were not altered after injury and suggests that FAIR protocols optimized to measure SCBF provide more value in the context of acute traumatic injury to the cord. T_1-relaxation time constants were strongly related to injury severity and had a larger extent of changes than either SCBF or DWI measures. These findings suggest that perfusion decreases in the spinal cord can be monitored non-invasively after injury, and multi-parametric MRI assessments of perfusion, diffusion, and relaxation capture unique features of the pathophysiology of preclinical injury.

[*]**Corresponding author at:** Zablocki VA Medical Center, Neuroscience Research Labs - Research 151, 5000 West National Ave, Milwaukee, WI 53295, seolee@mcw.edu.

Keywords

Spinal cord injury (SCI); arterial spin labeling (ASL); flow-sensitive alternating inversion recovery (FAIR); spinal cord blood flow (SCBF); T_1-relaxation time

1. Introduction

Spinal cord injury (SCI) is a devastating injury that can negatively affect quality of life [1]. Traumatic SCI immediately disrupts blood supply to the spinal cord, which can result in ischemia or hemorrhage that further damages the cord beyond the initial injury. Minimizing secondary injury by re-stablishing SCBF is advocated as a clinical recommendation for spinal cord trauma. The recommendations call for management of systemic blood pressure to maintain perfusion in the cord [2,3]. Thus, spinal cord blood flow (SCBF) may be one of the key features of SCI. However, techniques to monitor spinal cord perfusion non-invasively are limited. Traditional invasive methods to measure SCBF include radioactive microspheres and hydrogen clearing techniques [4–7], but these are not viable clinical solutions to evaluate disruptions in SCBF over time or with interventions. Recently, efforts to develop non-invasive techniques to measure SCBF have intensified, including measurements of perfusion with magnetic resonance imaging (MRI) using arterial spin labeling (ASL).

Perfusion MRI is a widely used technique in the brain and other organs, but these methods have not been routinely adopted to the spinal cord. Three previous studies have investigated the feasibility of monitoring SCBF using ASL in rodents using flow-sensitive alternating inversion recovery (FAIR) techniques [8–10]. Duhamel et al (2009) first demonstrated refinement of FAIR in the mouse cervical and lumbar cords, with disruption of SCBF after injury in a single animal [9]. In a rat model of cervical spondylotic myelopathy (CSM), FAIR demonstrated reductions in SCBF at the level of spinal cord compression and partial restoration after decompression surgery [10]. SCBF monitored with FAIR has also been demonstrated in the mouse lumbar cord in a model of multiple sclerosis to follow the clinical course of disease [11]. In summary, while it has been shown to be feasible to non-invasively measure SCBF in rodent models, particularly in the cervical and lumbar cord, there is a lack of reported data in the thoracic spinal cord, which is common for experimental SCI. Moreover, there is a lack of insight to the relationship between SCBF measured by MRI and injury severity or neurobehavioral outcomes after acute traumatic SCI. These features are essential to further understand the role of perfusion as a therapeutic target in the clinical management of SCI.

The goal of this study was to non-invasively measure quantitative SCBF at the thoracic lesion site (T10) using *in vivo* FAIR, and to examine the relationship between SCBF and neurological outcomes in a rat contusion SCI model. In addition to SCBF, it is unknown how injury might affect the dynamics of blood flow to the cord. In the rat, the spinal cord gray matter is fed primarily by sulcal arteries that branch off of the anterior spinal artery and penetrate through the ventral sulcus to supply much of the gray matter [12]. Traumatic injury may alter the arterial transit times (ATT) of blood to the spinal cord segment of

interest. Thus, we performed the FAIR acquisitions using a wide range of TI values to simultaneously estimate SCBF, ATT, and T_1. These metrics were compared to a separate spinal cord-optimized diffusion weighted imaging previously shown in the same model [13,14] to examine the relationship between perfusion and diffusion changes in the acutely injured thoracic spinal cord.

2. Materials and methods

2.1. Animals

Thirty-eight female Sprague-Dawley rats (age 8–10 weeks, weight 200–250 g) were used for this study. Rats were administered a sham (n=8), mild (n=10), moderate (n=10), or severe (n=10) contusion SCI at the T10 vertebral level. All animal procedures were approved by the Institutional Animal Care and Use Committees at the Medical College of Wisconsin and the Clement J. Zablocki Veterans Affairs Medical Center.

2.2. Spinal Cord Injury Procedure

Contusion SCI was induced in each rat using a weight drop apparatus. Animals were anesthetized with 4% inhalant isoflurane prior to the SCI procedure and were checked for leg flexion withdrawal and corneal reflexes, and then 2.5% isoflurane was maintained during the procedure. Using aseptic technique, an incision was made on the dorsal side of rat. A T10 laminectomy was performed exposing the spinal cord while keeping the dura intact. Using the NYU impactor device, a 10g steel rod was dropped from varying heights (12.5, 25, and 50 mm for mild, moderate, and severe, respectively) with a 2.5 mm diameter tip. Rats that received a sham injury underwent the same laminectomy procedure except for the weight drop. The animals were sutured closed and administered carprofen for pain for three subsequent days. Behavioral assessments of locomotor function were performed using the Basso, Beattie, Bresnahan (BBB) score [15,16] once every week by scoring hind limb function during rats freely exploring within a flat, 1-meter diameter open field for 4 minutes. BBB scoring was conducted independently from the MRI analysis.

2.3. Magnetic Resonance Imaging

In vivo MRI was performed 24 hours after injury on a Bruker 9.4 T Biospec System operating ParaVision version 6.0.1 software (Bruker Biospin, GmbH). A 9 cm diameter quadrature volume coil was used for transmission, and 4-channel surface coil for reception, centered at the injury epicenter at the T10 thoracic vertebrae. The animals were positioned supine in a custom head holder with a bite bar and ear bars to aid in minimizing motion artifacts. During imaging, respiration and temperature were continuously monitored. Although no respiratory gating was used, isoflurane was adjusted to achieve constant respiratory rate, typically 50–60 breaths per minute. Sagittal T_1-weighted images were used to position the slices at the epicenter of injury, defined by the position of the T10 laminectomy and confirmed by the presence of intramedullary edema and occasional hemorrhage within the spinal cord.

FAIR images were acquired using a four-shot echo planar imaging (EPI) acquisition (TE=18 ms, constant recovery time=3000 ms, field of view (FOV)=15.84×15.84 mm^2, spatial

resolution=0.165×0.165 mm^2, slice-thickness=2 mm). The FAIR pulse sequence consisted of slice-selective (SS) or non-slice-selective (NS) hyperbolic secant (sech) inversion pulses (Fig. 1A & B). Two different configurations of the inversion slice were performed using either single- or mutli-slice imaging (Fig. 1C). A single-slice inversion scheme used an axial inversion slice with a thickness of 4 mm centered at the imaging slice (1 mm inversion-to-imaging slice gap per side). The multi-slice inversion scheme consisted of an axial inversion slice with a thickness of 24.25 mm, centered at the full axial slice package consisting of ten, 2 mm thick slices with a gap of 0.25 mm, with the total imaging volume of 22.25 mm (= slice thickness 2 mm x 10 slices + 9 x slice gap 0.25 mm) and 1 mm inversion-to-imaging slice gap per side. For both schemes, ten images were acquired with inversion times (TI) of 50, 250, 500, 800, 1000, 1500, 2000, 3000, 5500, and 7500 ms with two repetitions of the selective and non-selective inversions. The multi-slice acquisitions used a single inversion pulse, and the delay between the acquisition of each slice was 30 ms, collected with interleaved slice ordering.

The diffusion weighted imaging (DWI) sequence, previously described by Skinner et al. [13], consisted of diffusion weighting at multiple diffusion-weighted factors (b-values) perpendicular and parallel to the spinal cord. For perpendicular diffusivity, b-values of 0, 200, 500, 1000, and 2000 s/mm^2 were used. For parallel measurements, a constant, high amplitude diffusion encoding (b=2000 s/mm^2) perpendicular to the cord was employed to simultaneously suppress or 'filter' fast-moving spins presumed to be non-axonal in addition to the parallel b-values of 0, 250, 500, 750, and 1000 s/mm^2. The DWI was acquired using a 4-shot EPI (TE=31 ms, TR=1600 ms, FOV=15.84×15.84 mm^2, spatial resolution=0.165×0.165 mm^2, slice-thickness=2 mm, NEX=4). Slices were positioned identical to those for the FAIR sequence.

2.4. Data Analysis

Spinal cord blood flow (SCBF) was quantified using two different models. The first equation is a biexponential FAIR model using multiple TI, which provides values for the non-slice-selective and slice-selective magnetization states with short TR, $M_{NS}(t)$ and $M_{SS}(t)$ [17].

$$\Delta M(TI) = M_{SS}(TI) - M_{NS}(TI)$$
$$= \frac{2M_0 \frac{f}{\lambda} \alpha_0 X(TR)}{\frac{1}{T_{1app}} - \frac{1}{T_{1a}}} \left(1 - e^{-\frac{TR}{T_{1a}}}\right) \left[\left(e^{-\frac{TI}{T_{1a}}} - e^{-\frac{TI}{T_{1app}}}\right) - (1 - 2\alpha_0) e^{-TI} \left(\frac{1}{T_{1a}} + \frac{1}{T_{1app}}\right) \left(e^{-\frac{\tau}{T_{1a}}} - e^{-\frac{\tau}{T_{1app}}}\right)\right]$$

In Equation 1, TI represents inversion recovery time, M_0 the magnetization of the equilibrium state, f the capillary blood flow (SCBF), α_0 the effective degree of inversion ($\alpha_0 \approx 0.95$) [18], T_{1app} an apparent longitudinal tissue relaxation time, T_{1a} the longitudinal relaxation time of blood (T_{1a}=2.38 s), τ the recovery time ($\tau \approx 3$s) and λ the blood-tissue partition coefficient ($\lambda \approx 0.9$) [19]. The X(TR) term accounts for the relaxation of blood during the constant recovery times. The same term in reference [17] assumes interleaved selective and non-selective inversion pulses, whereas this study used non-interleaved selective and non-selective inversion pulses with 4 EPI segments for each inversion. Therefore, this value was estimated using Bloch simulations of the full experimental design

of selective and non-selective ordering to obtain the magnetization state of blood for each TI. The second FAIR model equation uses a single TI but ignores the effect of ATT [9].

$$\Delta M(TI) = M_{NS}(TI) - M_{SS}(TI) = 2M_0\alpha_0\frac{f}{\lambda}\left(\frac{e^{-\frac{TI}{T_{1a}}} - e^{-\frac{TI}{T_{1app}}}}{\frac{1}{T_{1app}} - \frac{1}{T_{1a}}}\right)$$

This model has been previously validated for cervical and lumbar SCBF measurements with finite coil length, assuming blood velocities in small rodent animals are fast enough to ignore ATT in SCBF calculation. Therefore, Equation 2 was also tested for thoracic SCBF measurements along with Equation 1.

To quantify SCBF with both multiple and single TI configurations, T_{1app} is derived from slice-selective magnetization state $M_{SS}(t)$ using Equation 3 [8,9]. In addition to T_{1app}, spinal cord tissue T_1 is also separately estimated using Equation 3 but from non-slice-selective magnetization state $M_{NS}(t)$, which is considered as 'control' condition in FAIR method.

$$M(TI) = M_0\left(1 - 2\alpha_0 e^{-\frac{TI}{T_{1app}}}\right)$$

For multi-slice data, the time shift due to different acquisition times of each slice (30 ms) relative to the inversion time was taken into account.

From DWI, apparent diffusion coefficients were calculated separately perpendicular to and parallel to the cord with

$$S_i = S_0 \cdot e^{-b \cdot ADC}$$

where S_i is the diffusion-weighted signal, S_0 is the non-diffusion weighted signal, b is the b-value, and ADC is the estimated diffusivity. Perpendicular diffusivity ($ADC_\perp$) was estimated using b-values perpendicular to the cord, and parallel diffusivity ($fADC_\parallel$) is referred to as filtered axial diffusivity in this study since it was estimated from only parallel b-values with the perpendicular 'filter' component of the b-value neglected in the estimation [13]. All voxel-wise maps were computed in custom routines implemented in MATLAB (release: 2017a; The MathWorks, Inc., Natick, MA).

A region of interest analysis (ROI) was performed at the T10 lesion injury epicenter to obtain MRI metrics for subsequent analysis using ImageJ (version 2.0.0). For FAIR, the whole-cord ROIs were traced manually on the raw images having the discernable contrast between the spinal cord and surrounding CSF (TI=7500ms). For DWI, ROIs were first identified using semi-automated methods as described previously [20] on images with the largest perpendicular-diffusion weighting since the spinal cord is clearly depicted without signal from CSF or other tissues. These images were converted to maps of signal-to-noise (SNR) by dividing each voxel by the standard deviation of a region of noise. The SNR

images were thresholded at an SNR of 15 which was determined empirically by identifying the value that best segmented the spinal cord from the noise [20]. The same SNR value was used for all animals. Manual corrections of the segmented images were also occasionally performed to refine ROIs to exclude signal from residual fat not fully suppressed.

2.5. Statistical Analysis

All statistical analysis was conducted using the Statistical Package for Social Sciences (SPSS version 26; IBM Corp., Armonk, NY). A one-way ANOVA was used to identify differences in MRI metrics among groups of different injury severities, and a Bonferroni post-hoc test was performed to identify individual group differences. Pearson's product moment correlations were performed to determine the linear relationships between MR metrics and BBB scores. Additional multiple linear regression was conducted to examine the independence of MR parameters in predicting later BBB scores. For a more accurate representation of the results, correlations and multiple linear regressions are performed and reported both with and without sham animals since they may an undue influence on the resulting correlations due to ceiling effects and distributions in BBB scores compared to injured animals.

3. Results

3.1. Single-slice FAIR at the lesion epicenter

Representative single-slice inversion recovery images across 10 different TI are shown from a sham-injured animal at the thoracic T10 level (Fig. 2). A signal difference in spinal cord tissue between the slice-selective (SS) and non-slice-selective (NS) inversions can be observed across TI. The signal in the posterior spinal artery is clearly evident between two conditions. In a gray matter ROI, the signal is shown as a function of TI (Fig. 2C) and the difference in signal between the SS and NS conditions reflects perfusion contrast between 1000 and 3000 ms.

The sham animals were investigated in additional detail to probe the perfusion dynamics and variability in SCBF estimates (Fig. 3). The normalized perfusion weighted contrast ($\Delta M/M_0$) within the posterior spinal artery, the most readily visualized large spinal cord artery in the images, had a sharp increase in contrast at TI=800 ms. In the gray matter in the same animals, perfusion contrast increased with a short lag compared to the artery, increasing at TI=1000 ms, peaking at 2000ms and decreasing thereafter. SCBF was quantified from the perfusion contrast using either the multi-TI data or at each TI (Fig. 3B) from the gray matter, both using the estimated T_{1app} from the slice-selective inversion recovery. The SCBF estimates for multi-TI analysis revealed SCBF estimates of 235 ± 95 mL/100 g/min. At each TI analyzed separately, SCBF estimates varied. At TI=1500ms, SCBF had similar values as the multi-TI estimates and had the lowest variability (coefficient of variation (CoV) of 27%) compared to other single- or the multi-TI condition (CoV=40%). It is noted that TI=1500 coincides with the lowest CSF signal, suggesting the reduction of CSF signal diminishes background artifacts that can add variability to SCBF estimates, and TI=1500 ms was used for further analysis.

SCBF maps are shown for a sham and severely injured animal at the site of injury (Fig. 4). Compared to the sham animal, the severe injury caused a clear disruption in the normal cord anatomy with a small amount of hemorrhage in this particular animal. A loss of gray and white matter contrast was evident along with increased T_1 values throughout the cord. SCBF contrast is diminished in the cord. Due to the loss of clear contrast that precluded reliable gray matter regions of interest, manual whole-cord ROIs were used for subsequent analysis guided by the border between the tissue and CSF. One animal with mild injury exhibited extremely high $\Delta M/M_0$ values due to a severe motion artifact and was excluded. Therefore, a total of thirty-seven (8 sham, 9 mild, 10 moderate, and 10 severe) were included for the following group comparisons.

The perfusion contrast ($\Delta M/M_0$) grouped by injury severity is shown in figure 5 with the whole-cord ROI analysis at the lesion site. Each injury group qualitatively showed similar perfusion contrast across different inversion times with a similar increase in contrast between 800 and 1000 ms. Perfusion contrast was diminished for the injured animals. Estimated ATT values (Fig. 5B) did not appreciably or reliably differ across injury severities as assessed by a one-way ANOVA ($F(3,33)=0.299$, $p=0.826$). T_1 (Fig. 5C) consistently increased with greater injury severity and had a significant effect by group ($F(3,33)=34.986$, $p<0.001$). Pairwise group post-hoc comparisons showed significant differences in T_1 for the sham vs mild ($p<0.001$), sham vs moderate ($p=0.001$), sham vs severe ($p<0.001$), and mild vs severe($p=0.027$) groups. SCBF quantified with multiple TI and single-TI analysis revealed similar trends and both are shown for completeness (Fig. 5D & 5E). Decreasing SCBF was seen with greater injury severity although the trends across groups were somewhat variable. With single-TI configuration, a one-way ANOVA revealed a significant effect of injury severity on SCBF ($F(3,33)=3.175$, $p=0.037$), and a post-hoc group comparison showed significant difference for the sham vs severe ($p=0.028$). Single-TI analysis yielded mean SCBF values of 168, 113, 109, and 82 mL/100 g/min in the sham, mild, moderate, and severe groups, respectively, equating to reductions of SCBF of 33%, 35%, and 51% reductions compared to the sham group. Similar to the gray matter analysis, the whole-cord ROI analysis in the sham group showed a reduction in variability in the single-TI analysis (CoV=37%) compared to the multi-TI analysis (58%), with similar trends of reduced variability across all the groups. [Insert Figure 5 here]

3.2. DWI at the lesion epicenter

Maps of filtered parallel apparent diffusivity ($fADC_{\parallel}$) showed the characteristic pattern of a contusion injury (Fig. 6A) with a decrease in $fADC_{\parallel}$ in the central portion of the cord surrounded by a relatively preserved region of higher $fADC_{\parallel}$ along thespinal cord periphery. Additionally, a midline cavitation is also evident in the $fADC_{\parallel}$ map which is also evident in the map of perpendicular diffusivity ($ADC_{\perp}$), although cavitation does not always occur. Across all animals, a trend of decreasing $fADC_{\parallel}$ values were observed at the lesion epicenter with greater severity (Fig. 6B), consistent with previous results [13]. A one-way ANOVA test revealed a significant effect of injury severity for parallel diffusivity $fADC_{\parallel}$ ($F(3,33)=3.863$, $p=0.018$), while there were no significant effects of injury severities for perpendicular diffusivity $ADC_{\perp}$ ($F(3,27)=1.857$, $p=0.156$). A Bonferroni-corrected post-hoc test revealed a significant difference of $fADC_{\parallel}$ between the sham vs severe ($p=0.020$) pair.

3.3. Multi-slice FAIR and DWI

The multi-slice results from perfusion and diffusion measures across the injury also used a whole-cord ROI analysis (Fig. 7). Inversion recovery images (TI=7500 ms) are shown from one animal from each of the injury groups to demonstrate the image quality and qualitative evaluation of anatomical changes (Fig. 7A). Using multi-TI analysis, ATT values were estimated across slices and did not appreciably or reliably differ across injury severities (Fig. 7B), similar to the results of the single-slice data. SCBF with single-TI analysis revealed a general decrease at the lesion epicenter (Fig. 7C), and significant effects of injury severity were evident at the slice centered on the lesion ($F(3,30)=4.594$, $p=0.009$) and one slice (2 mm) above the injury slice ($F(3,26)=3.076$, $p=0.045$). A trend of decreased SCBF values was seen for all animals at the slices further below the injury, but this is believed to be a reflection of the larger gray matter to white matter content across the different slices. $fADC_{\parallel}$ demonstrated a more focal change at the lesion epicenter ($F(3,33)=3.863$, $p=0.018$), but there was no significant differences away from the injury site (Fig. 7D). $ADC_{\perp}$ did not change across any of the slices (Fig. 7E). Finally, T_1 demonstrated a broader response to injury, with a significant effect of injury at the lesion epicenter ($F(3,33)=7.001$, $p=0.001$) as well as one slice (2 mm) below ($F(3,33)=3.320$, $p=0.032$) and above ($F(3,33)=3.610$, $p=0.023$) the injury slice (Fig. 7F).

3.4. Relationships between MR metrics and BBB scores

BBB scores were assessed at 2 days post-injury and weekly thereafter up to 28 days after injury (Fig. 8). Prediction of the BBB outcome scores at 28 days post-injury was evaluated using the acute (24 hours) post-injury MRI metrics. Four animals failing to survive until 28 days after injury were excluded (1 moderate and 3 severe), and a total 33 animals underwent prediction analysis. A one-way ANOVA of final BBB scores (28 days post-injury) showed significant differences for the different injury severities ($F(3,33)=58.820$, $p<0.001$).

Both SCBF and T_1 showed strong positive and negative correlations with BBB scores, respectively (Table 1), and analysis was performed with both sham animals included and excluded and using only the single-slice results at the lesion epicenter. T_1 was most strongly associated with outcomes and was significantly related to BBB scores both with and without sham animals. For DWI, $fADC_{\parallel}$ showed a significant correlation with BBB both with and without the sham group included. The strength of the relationship between $ADC_{\perp}$ and BBB score was lower than that of $fADC_{\parallel}$ and showed a significant correlation with BBB only when the sham group was excluded. Lastly, SCBF had a lower relationship with BBB scores than either $fADC_{\parallel}$ or T_1 and was significantly related to BBB scores only with sham animals included, which reflects the reduction of SCBF with injury compared to sham animals but without consistent trends related to the degree of severity. Multiple linear regression was performed with three parameters, SCBF, T_1 and $fADC_{\parallel}$ to evaluate their independence as predictors of outcome. With shams included ($F(3,29)=24.127$, $p<0.001$, $R^2_{adjusted}=0.684$) or excluded ($F(3,21)=5.576$, $p=0.006$, $R^2_{adjusted}=0.364$), the strength of the relationship between all MRI metrics and BBB scores did not appreciably differ compared to the individual pairwise assessments. T_1 was the only independent and significant predictor of eventual outcome either with sham animals included (T_1: $\beta=-0.783$, $t=-5.508$, $p<0.001$; SCBF: $\beta=0.076$, $t=0.656$, $p=0.517$; $fADC_{\parallel}$: $\beta=0.033$, $t=0.265$, $p=0.793$) or sham animals

excluded (T_1: β=−0.552, t=−2.331, p=0.030; $fADC_{||}$: β=0.147, t=0.673, p=0.508; SCBF: β=0.040, t=0.215, p=0.832).

4. Discussion

In this study evaluating FAIR as a biomarker for SCI injury severity and a predictor of outcome, we first adopted the conventional single-slice FAIR sequence [21] among animals with differing injury severities to assess the effects at the lesion epicenter. Overall, the results demonstrate that SCBF is altered after thoracic contusion injury, but DWI and T_1 exhibited more consistent relationships with injury severity and predictors of neurological outcome.

4.1. SCBF

After a traumatic SCI, disruption of the vasculature is an early event of the primary injury, and is known to alter blood flow and oxygen delivery as shown through terminal or invasive procedures [22–24]. Furthermore, the edema and swelling of the cord can cause further reductions in SCBF resulting in ischemia and impaired flow, which can exacerbate the degree and extent of damage (i.e. secondary injury) [24,25]. In agreement with previous evidence, we observed reduced SCBF at the epicenter of contusion. Although literature on quantifying SCBF using the FAIR sequence is sparse, there have previously been efforts to accomplish this goal: cervical and lumbar spinal cord in mice [8,9], and cervical spondylotic myelopathy in rat [10]. For example, Duhamel et al. quantified the absolute SCBF with FAIR at the lumbar L1 level (gray matter: 285 mL/100 g/min; white matter: 100 mL/100 g/min) as well as at the cervical C3 level (gray matter: 310 mL/100 g/min; white matter: 121 23 mL/100 g/min). Our results in the sham rat cord (gray matter: 226 mL/100 g/min; white matter: 133 mL/100 g/min) are within a comparable range and yield an approximate WM/GM SCBF ratio of 58% comparable to 54% reported using the hydrogen clearance method [6]. Similarly, the variability in SCBF estimated in sham animals at a single TI in the gray matter (CoV=27%) also compared favorably with previous cervical and lumbar FAIR studies (CoV=25–32%) [8,9]. A study that quantified SCBF using FAIR in a cervical spondylotic myelopathy rat model also reported a comparable SCBF value (~160 mL/100 g/min) 24 hours after decompression surgery. Furthermore, compared to the previous works by Duhamel et al. [8,9], our target region of interest was thoracic level, and in addition to ASL image quality being inevitably more susceptible to motion artifact due to respiration, differences in the relative amounts of gray and white matter are expected to modulate whole-cord SCBF values. Disruption of the normal anatomy after a contusion injury also limited the ability to resolve white and gray matter.

Currently, the most accurate method to measure blood flow is an invasive measure such as radioactive microsphere [4,5], autoradiography [26,27], or hydrogen clearance [6,7] with which SCBF values were generally estimated at less than 100 mL/100 g/min. Interestingly, SCBF measured with ASL appears to consistently report much higher SCBF at a few hundred mL/100 g/min, compared to SCBF measured by invasive techniques. This overestimation of SCBF may be, in part, due to anesthesia conditions [8,9]. In a continuous ASL study, cerebral blood flow was found to be markedly increased when rats

were anesthetized with isoflurane, than with either pentobarbital or fentanyl, which might result in an overestimation of blood flow [28]. Additionally, the contribution of vascular signal cannot be ruled out since this study did not use vascular suppression techniques that minimize the expected overestimates of perfusion [29]. Nevertheless, the estimation of SCBF in our study was applied similarly over all animals to compare relative changes after injury between groups.

In these results, SCBF showed the lowest variability across sham animals at TI=1500ms compared to other inversion times or using the full multi-TI analysis. This finding is in accord with several prior mouse and rat studies using the FAIR technique in the spinal cord. With the chosen recovery time of 3000 ms in this study, the TI=1500 ms corresponds to the lowest CSF signal (i.e. null). Given the relatively low contribution of perfusion to the total signal, ASL methods are often challenged by artifacts from other tissues, and FAIR inherently includes this background-suppression effects. Our results in the sham animals demonstrate the importance of reducing artifacts while maintaining appropriate delays for the tissue under interest. These results suggest that an explicit inversion time chosen to null CSF for future FAIR studies in the spinal cord is likely improve accuracy of SCBF estimates, and in the rodent, TI=1500 ms was also sufficient to maintain high perfusion contrast. Given the lack of ATT changes after injury, this metric does not appear to provide sensitivity to the injury and further implicates the choice of a single inversion time. The multiple inversion times also limited the use of respiratory gating in this study, which is critical for spinal cord imaging, especially in the thoracic cord. A single inversion time will be more compatible with prospective respiratory gating strategies [9]. Notably, with 2 repeats of the full range of inversion times in this study, only 2 pairs of images were used for estimation of SCBF at a single TI, and many more repetitions would be recommended for future studies to enhance voxelwise SCBF maps and improve the temporal signal to noise (tSNR). Our FAIR acquisition was also limited by the lack of a second pulse to saturate the blood signal known as Q2TIPS, which improves imaging for multi-slice acquisitions. Several studies using this protocol has previously verified the feasibility of multi-slice ASL scan at the rat cervical or lumbar spinal cord [11,30,31].

Despite perfusion ASL of the spinal cord shown in this and previous studies, non-invasive imaging of spinal cord perfusion has not yet translated to reliable monitoring for the human spinal cord. Spinal cord perfusion after traumatic SCI is a feature and therapeutic target of high importance. Clinical guidelines recommend maintenance of spinal cord perfusion in the initial 7 days post injury through control of mean arterial pressure [32]. Invasive probes implanted into the epidural space of the spinal cord have demonstrated the role of spinal cord perfusion pressure in acute animal studies [32], and human SCI studies have demonstrated the impact of maintaining spinal cord perfusion hemodynamics [33,34]. Laser speckle contrast imaging has also been used to describe patterns of SCBF in the acute stage of human SCI in the context of inter-operative imaging [35] in which a low SCBF necrosis-penumbra pattern was observed in thoracic injury or with a ‘patchy-pattern’ with a mixture of irregular low, intermediate, and high SCBF values. In our study, mean SCBF values were estimated in the cross-sectional whole cord. Along with clinically compatible perfusion ASL methods for the spinal cord, improvements in SNR and resolution are also needed to identify whether different perfusion patterns emerge in human SCI, and whether

these perfusion changes relate to hemorrhage or other pathologic features that MRI is exceptional at detecting non-invasively.

4.2. T_1

We also evaluated quantitative T_1 as a biomarker of injury severity. With increasing severity, an increasing trend of T_1 was evident (Fig. 5C). Acute SCI involves both vasogenic and cytotoxic edema at the initial injury site, which accumulates excess fluid at the site of contusion impact [36] and lengthens the T_1-relaxation time constant of the injured spinal cord. While it is well-known that acute neurological injury causes changes in T_1 and T_1-weighted imaging is part of the most clinical imaging repertoires for trauma, the relationship between SCI and quantitative T_1 after injury has not been examined. Increased T_1 values of spinal cord white matter have been noted caudal to the injury site in rat SCI [37], implicating the role of myelin-bound cholesterol in addition to edema. In summary, the increased T_1 after SCI and significant relationship to neurological outcome may make T_1 useful as a clinical marker of injury severity. One complication is the presence of blood in the tissue which is potentially a source of artifact and variability using echo planar imaging. Many other MRI techniques are available to quantify T_1, which may have greater utility for the challenges of imaging the injured cord. Reductions in acquisition time or alternative and efficient methods of quantitative T_1 mapping are necessary prior to future translation. Given these results along with the variety of pulse sequences to measure T_1, methods suitable for acute clinical examination may have important utility in human SCI.

4.3. Diffusion Weighted Imaging

In rodent experimental models of SCI, diffusion imaging and diffusion tensor imaging in particular have been widely used, with consistent findings indicating a decrease in parallel diffusivity at the lesion site. This study built on similar prior work to reduce the effect of edema on the resulting DWI indices using a diffusion ‘filter’ to suppress extracellular and other signals that can confound interpretation including CSF or perfusion effects. It has previously been reported that $fADC_{\parallel}$ is a sensitive predictive biomarker in the acute SCI rat model using a whole-cord spectroscopic sequence [13] and EPI-based readouts [14]. Our study confirmed that there is significant decline of $fADC_{\parallel}$ with increasing severity at 1 day post injury with a significant relationship with BBB scores at 28 days post injury (R^2=0.270, p=0.002), consistent with previous studies in the same injury model. In a direct comparison using multiple linear regression, however, quantitative T_1 outperformed SCBF and $fADC_{\parallel}$ as a predictor of final BBB score. Thus, while DWI has strong associations with the underlying pathology, a multi-parametric MRI protocol is likely to be most advantageous to predict outcomes given the inherent variability of human SCI and presence of multiple coincident pathologies. Interestingly, $ADC_{\perp}$ showed a statistically significant correlation with final BBB score when sham animals were excluded (R^2=0.193, p=0.028), noting the strength of the relationship was lower than either $fADC_{\parallel}$ or T_1. Previous animal studies have consistently shown that $ADC_{\perp}$ or radial diffusivity is not a strong maker of acute injury, particularly compared to $fADC_{\parallel}$ [13].

4.4. Limitations

The FAIR sequence used for this study included 10 inversion times in consideration of possible variations in ATT, which resulted in a long scan time (~18 mins) and several sub-optimal tradeoffs in the MRI acquisition. As discussed above, using a single or reduced set of TI times is likely the preferred strategy for future studies. Additionally, this study used an EPI readout in the axial plane. EPI is advantageous for fast imaging and is routinely used for spinal cord imaging, but injury disrupts the normal cord morphology and intramedullary hemorrhage is common pathology which both affect image quality and can contribute to quantification errors. Specifically, the presence of intramedullary hemorrhage in the injury model may introduce variability of SCBF estimates, and spin-echo based readout methods may diminish this variability. In the cervical rat spinal cord, recent work has shown that sagittal imaging in combination with fast spin echo readout provided high-quality SCBF maps to reveal the longitudinal extent of perfusion deficits using pseudo-continuous labelling [38]. This approach has not been evaluated in the thoracic spinal cord, but it may offer improvements in accuracy. Since sagittal imaging is generally preferred in the clinical setting to diagnose and detect damage to the human spinal cord, optimization of FAIR with alternative imaging readouts may prove to have better translational value. Likewise, other ASL variants such as velocity selective tagging may be useful for greater spatial coverage in SCI. Furthermore, validation with gold-standard markers of perfusion and histological markers of capillary integrity or density are also needed to correlate the MR-based SCBF measures and would be beneficial to interpret the results more comprehensively in the context of microscopic damage to the cord.

5. Conclusion

In this study, quantitative SCBF, DWI, and T_1 maps were calculated at the thoracic T10 level in rat after acute SCI. The FAIR EPI sequence shows potential for use in evaluating spinal cord injury, and the relationship between SCBF and behavioral outcomes were studied in the acute phase of SCI in rats. Decreasing SCBF was evident after injury, but a consistent relationship with injury severity was not observed. Notably, injured animals did not exhibit changes in perfusion delays quantified as ATT. The results suggest that FAIR methods optimized strictly for SCBF estimation in the context of acute SCI are more beneficial than those to measure transit delays. Quantitative T_1 values also outperformed either SCBF and $fADC_{\|}$ as reliable predictors of behavioral outcomes in rodent SCI, but also showed a greater extent of changes compared to either perfusion or diffusion markers. The multi-parametric MRI metrics and outcomes in this study may prove useful in future preclinical studies to evaluate therapies that target one or more of the pathologies caused by trauma to the spinal cord in the pursuit of treatments for SCI.

Acknowledgements

This project was funded by the National Institute of Neurological Disorders and Stroke of the National Institutes of Health under Award Number R01NS109090. We thank Matt Runquist and Kathleen Yin for their assistance with MRI.

Abbreviations:

ADC $_{\perp}$
Perpendicular diffusivity

ASL
Arterial spin labeling

BBB
Basso, Beattie, Bresnahan locomotor scoring

CSM
Cervical spondylotic myelopathy

DWI
Diffusion-weighted imaging

EPI
Echo-planar imaging

fADC $_{\parallel}$
Filtered parallel diffusivity

FAIR
Flow-alternating sensitive inversion recovery

NS
Non-slice-selective

ROI
Region of interest

SCBF
Spinal cord blood flow

SCI
Spinal cord injury

SNR
Signal-to-noise ratio

SS
Slice-selective

TI
Inversion time

REFERENCES

[1]. Lynch J, Cahalan R. The impact of spinal cord injury on the quality of life of primary family caregivers: A literature review. Spinal Cord 2017;55:964–78. 10.1038/sc.2017.56. [PubMed: 28653672]

[2]. Izumi S, Okada K, Hasegawa T, Omura A, Munakata H, Matsumori M, et al. Augmentation of systemic blood pressure during spinal cord ischemia to prevent postoperative paraplegia after aortic surgery in a rabbit model. J Thorac Cardiovasc Surg 2010;139:1261–8. 10.1016/j.jtcvs.2009.08.038. [PubMed: 19910005]

[3]. Kise Y, Kuniyoshi Y, Inafuku H, Nagano T, Hirayasu T, Yamashiro S. Directly measuring spinal cord blood flow and spinal cord perfusion pressure via the collateral network: Correlations with changes in systemic blood pressure. J Thorac Cardiovasc Surg 2015;149:360–6. 10.1016/j.jtcvs.2014.09.121. [PubMed: 25524689]

[4]. Wallace MC, Tator CH. Spinal cord blood flow measured with microspheres following spinal cord injury in the rat. Can J Neurol Sci 1986;13:91–6. 10.1017/S0317167100035976. [PubMed: 3719472]

[5]. Hickey R, Albin MS, Bunegin L, Gelineau J. Autoregulation of spinal cord flow: is the spinal cord a microcosm of the brain? Stroke 1986;17:1183–9. [PubMed: 3810718]

[6]. Rubinstein A, Arbit E. Spinal cord blood flow in the rat under normal physiological conditions. Neurosurgery 1990;27:882–6. 10.1227/00006123-199012000-00004. [PubMed: 2274128]

[7]. Guha A, Tator CH, Rochon J. Spinal cord blood flow and systemic blood pressure after experimental spinal cord injury in rats. Stroke 1989;20:372–7. 10.1161/01.STR.20.3.372. [PubMed: 2922776]

[8]. Duhamel G, Callot V, Cozzone PJ, Kober F. Spinal cord blood flow measurement by arterial spin labeling. Magn Reson Med 2008;59:846–54. 10.1002/mrm.21567. [PubMed: 18383283]

[9]. Duhamel G, Callot V, Decherchi P, Le Fur Y, Marqueste T, Cozzone PJ, et al. Mouse lumbar and cervical spinal cord blood flow measurements by arterial spin labeling: Sensitivity optimization and first application. Magn Reson Med 2009;62:430–9. 10.1002/mrm.22015. [PubMed: 19526492]

[10]. Karadimas SK, Laliberte AM, Tetreault L, Chung YS, Arnold P, Foltz WD, et al. Riluzole blocks perioperative ischemia-reperfusion injury and enhances postdecompression outcomes in cervical spondylotic myelopathy. Sci Transl Med 2015;7:316ra194–316ra194. 10.1126/scitranslmed.aac6524.

[11]. Desai RA, Davies AL, Del Rossi N, Tachrount M, Dyson A, Gustavson B, et al. Nimodipine Reduces Dysfunction and Demyelination in Models of Multiple Sclerosis. Ann Neurol 2020:1–14. 10.1002/ana.25749.

[12]. Mazensky D, Flesarova S, Sulla I. Arterial Blood Supply to the Spinal Cord in Animal Models of Spinal Cord Injury. A Review. Anat Rec 2017;300:2091–106. 10.1002/ar.23694.

[13]. Skinner NP, Kurpad SN, Schmit BD, Tugan Muftuler L, Budde MD. Rapid in vivo detection of rat spinal cord injury with double-diffusion-encoded magnetic resonance spectroscopy. Magn Reson Med 2016;00:1–11. 10.1002/mrm.26243.

[14]. Wilkins N, Skinner NP, Motovylyak A, Schmit BD, Kurpad S, Budde MD. Evolution of Magnetic Resonance Imaging as Predictors and Correlates of Functional Outcome after Spinal Cord Contusion Injury in the Rat. J Neurotrauma 2020;37:889–98. 10.1089/neu.2019.6731. [PubMed: 31830856]

[15]. Basso DM, Beattie MS, Bresnahan JC. Graded histological and locomotor outcomes after spinal cord contusion using the NYU weight-drop device versus transection. Exp Neurol 1996;139:244–56. 10.1006/exnr.1996.0098. [PubMed: 8654527]

[16]. Basso DM, Beattie MS, Bresnahan JC. A Sensitive and Reliable Locomotor Rating Scale for Open Field Testing in Rats. J Neurotrauma 1995;12:1–21. 10.1089/neu.1995.12.1. [PubMed: 7783230]

[17]. Pell GS, Thomas DL, Lythgoe MF, Calamante F, Howseman AM, Gadian DG, et al. Implementation of quantitative FAIR perfusion imaging with a short repetition time in time-course studies. Magn Reson Med 1999;41:829–40. [PubMed: 10332861]

[18]. Harteveld AA, de Boer A, Franklin SL, Leiner T, van Stralen M, Bos C. Comparison of multi-delay FAIR and pCASL labeling approaches for renal perfusion quantification at 3T MRI. Magn Reson Mater Physics, Biol Med 2020;33:81–94. 10.1007/s10334-019-00806-7.

[19]. Herscovitch P, Raichle ME. What is the correct value for the brain-blood partition coefficient for water? J Cereb Blood Flow Metab 1985;5:65–9. 10.1038/jcbfm.1985.9. [PubMed: 3871783]

[20]. Budde MD, Skinner NP, Tugan Muftuler L, Schmit BD, Kurpad SN. Optimizing filter-probe diffusion weighting in the rat spinal cord for human translation. Front Neurosci 2017;11:1–13. 10.3389/fnins.2017.00706. [PubMed: 28154520]

[21]. Kim SG. Quantification of Relative Cerebral Blood-Flow Change by Flow-Sensitive Alternating Inversion-Recovery (FAIR) Technique - Application to Functional Mapping. Magn Reson Med 1995;34:293–301. 10.1002/mrm.1910340303. [PubMed: 7500865]

[22]. Tator CH, Koyanagi I. Vascular mechanisms in the pathophysiology of human spinal cord injury. J Neurosurg 2009;86:483–92. 10.3171/jns.1997.86.3.0483.

[23]. Muradov JM, Hagg T. Intravenous Infusion of Magnesium Chloride Improves Epicenter Blood Flow during the Acute Stage of Contusive Spinal Cord Injury in Rats. J Neurotrauma 2013;30:840–52. 10.1089/neu.2012.2670. [PubMed: 23302047]

[24]. Popa C, Popa F, Grigorean VT, Onose G, Sandu AM, Popescu M, et al. Vascular dysfunctions following spinal cord injury. J Med Life 2010;3:275–85. [PubMed: 20945818]

[25]. Leonard AV, Thornton E, Vink R. The Relative Contribution of Edema and Hemorrhage to Raised Intrathecal Pressure after Traumatic Spinal Cord Injury. J Neurotrauma 2014;32:397–402. 10.1089/neu.2014.3543.

[26]. Sandler AN, Tator CH. Regional spinal cord blood flow in primates. J Neurosurg 1976;45:647–59. 10.3171/jns.1976.45.6.0647. [PubMed: 824417]

[27]. Holtz A, Nystrom B, Gerdin B. Regulation of spinal cord blood flow in the rat as measured by quantitative autoradiography. Acta Physiol Scand 1988;133:485–93. 10.1111/j.1748-1716.1988.tb08432.x. [PubMed: 3227934]

[28]. Hendrich KS, Kochanek PM, Melick JA, Schiding JK, Statler KD, Williams DS, et al. Cerebral perfusion during anesthesia with fentanyl, isoflurane, or pentobarbital in normal rats studied by arterial spin-labeled MRI. Magn Reson Med 2001;46:202–6. 10.1002/mrm.1178. [PubMed: 11443729]

[29]. Wang J, Alsop DC, Song HK, Maldjian JA, Tang K, Salvucci AE, et al. Arterial transit time imaging with flow encoding arterial spin tagging (FEAST). Magn Reson Med 2003;50:599–607. 10.1002/mrm.10559. [PubMed: 12939768]

[30]. Tachrount M, Davies A, Desai R, Smith K, Thomas D, Golay X, et al. Quantitative rat lumbar spinal cord blood flow measurements using multi-slice arterial spin labelling at 9.4T. Proc Intl Soc Mag Reson Med 2015;23:537.

[31]. Duhamel G, Marqueste T, Sdika M, Tachrount M, Decherchi P, Cozzone P, et al. Vascular Alterations and Recruitment in Spinal Cord Injury Revealed by Multislice Arterial Spin Labeling (ASL) Perfusion Imaging. Proc Intl Soc Mag Reson Med 2010;18:442.

[32]. Walters BC, Hadley MN, Hurlbert RJ, Aarabi B, Dhall SS, Gelb DE, et al. Guidelines for the management of acute cervical spine and spinal cord injuries: 2013 update. Neurosurgery 2013;60:82–91. 10.1227/01.neu.0000430319.32247.7f. [PubMed: 23839357]

[33]. Werndle MC, Saadoun S, Phang I, Czosnyka M, Varsos GV., Czosnyka ZH, et al. Monitoring of spinal cord perfusion pressure in acute spinal cord injury: Initial findings of the injured spinal cord pressure Evaluation Study*. Crit Care Med 2014;42:646–55. 10.1097/CCM.0000000000000028. [PubMed: 24231762]

[34]. Squair JW, Bélanger LM, Tsang A, Ritchie L, Mac-Thiong JM, Parent S, et al. Spinal cord perfusion pressure predicts neurologic recovery in acute spinal cord injury. Neurology 2017;89:1660–7. 10.1212/WNL.0000000000004519. [PubMed: 28916535]

[35]. Gallagher MJ, Hogg FRA, Zoumprouli A, Papadopoulos MC, Saadoun S. Spinal Cord Blood Flow in Patients with Acute Spinal Cord Injuries. J Neurotrauma 2018;36:919–29. 10.1089/neu.2018.5961. [PubMed: 30351245]

[36]. Rowland JW, Hawryluk GWJ, Kwon B, Fehlings MG. Current status of acute spinal cord injury pathophysiology and emerging therapies: promise on the horizon. Neurosurg Focus 2008;25:E2. 10.3171/foc.2008.25.11.e2.

[37]. Narayana P, Abbe R, Liu S-J, Johnston D. Does loss of gray- and white-matter contrast in injured spinal cord signify secondary injury? In vivo longitudinal MRI studies. Magn Reson Med 1999;41:315–20. [PubMed: 10080279]

[38]. Meyer B, Hirschler L, Warnking J, Barbier E, Budde M. Preclinical Spinal Cord Perfusion Imaging with Pseudo-Continuous Arterial Spin Labeling. Proc Intl Soc Mag Reson Med 2020;28:177.

Seongtaek Lee:

Conceptualization, Methodology, Software, Validation, Formal analysis, Investigation, Data Curation, Writing – Original Draft Preparation & Editing, Visualization, Re-analysis and Manuscript Revision.

Natasha Wilkins:

Methodology, Investigation, Resources, Data curation, Manuscript Revision.

Brain Schmit:

Conceptualization, Methodology, Writing – Review and Editing, Manuscript Revision.

Shekar N. Kurpad:

Conceptualization, Methodology, Writing – Review and Editing, , Manuscript Revision.

Matthew Budde:

Conceptualization, Methodology, Validation, Writing – Review and Editing, Supervision, Funding acquisition, Re-analysis and Manuscript Revision.

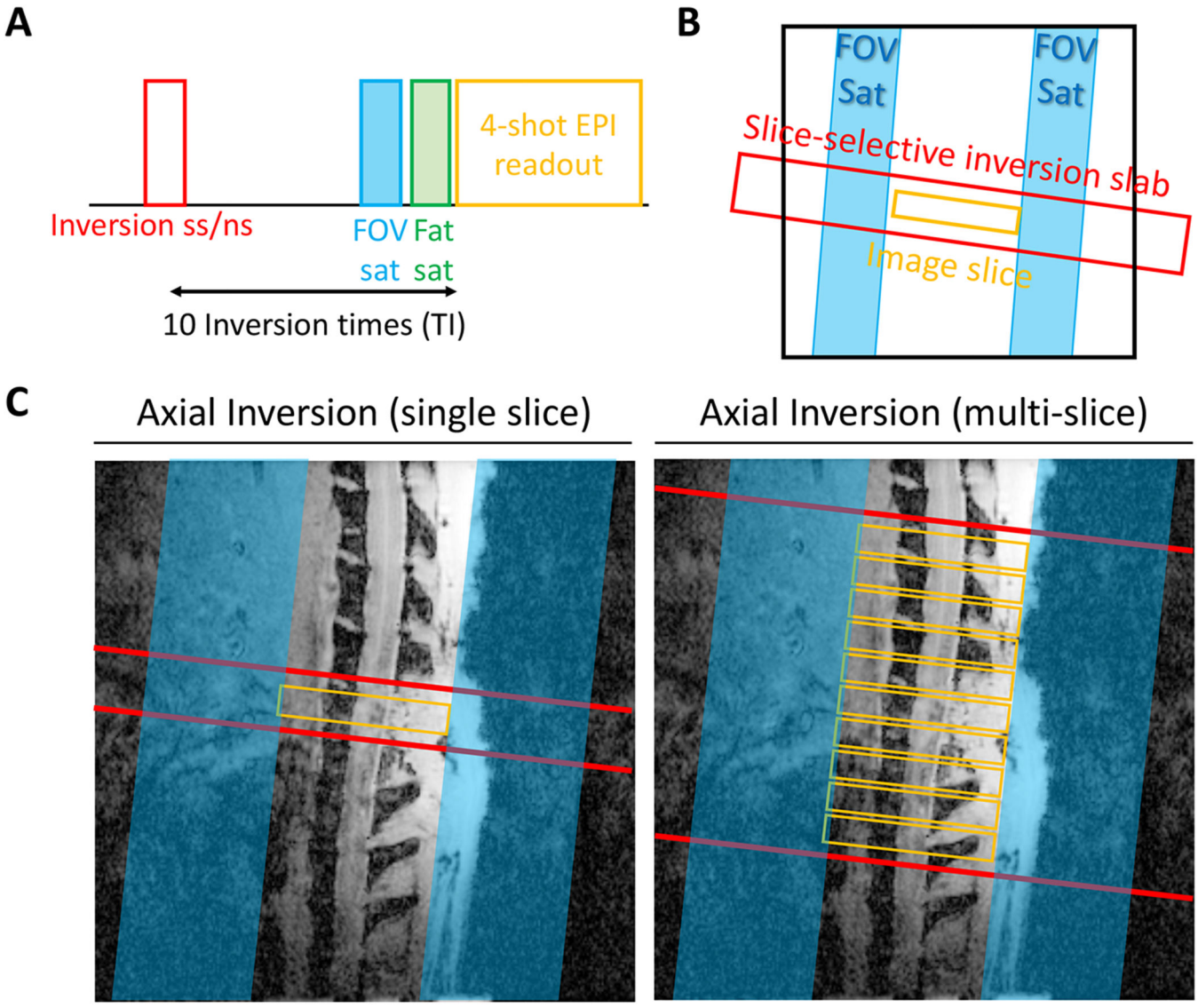

Figure 1.

Experimental inversion schemes. (A) Sequence diagram and (B) slice positioning of FAIR, including an inversion-recovery with either slice-selective or non-slice-selective inversion pulses. (C) Both single- and multi-slice variants were evaluated. FOV saturation slabs suppress unwanted signals outside the cord along and a chemical-shift fat-selective saturation module.

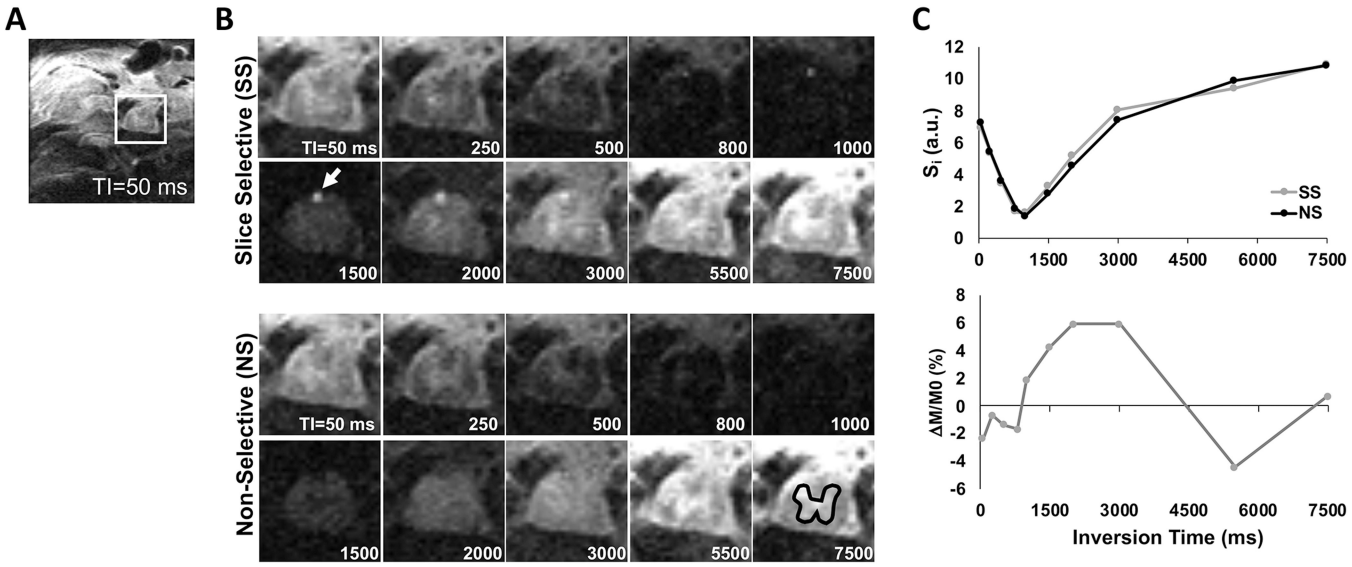

Figure 2.

Representative single-slice inversion recovery images of a sham animal. (A) Inversion recovery image (TI=50 ms) showing the full FOV in the thoracic cord. (B) Inversion recovery images across varying TI showing the change in contrast, highlighting the posterior spinal artery (arrow) and a gray matter ROI (black). (C) Signal intensity (S_i; top) and perfusion weighted signal (ΔM/M0; bottom**)** from the gray matter ROI reveal the change in perfusion contrast across different inversion times (TI).

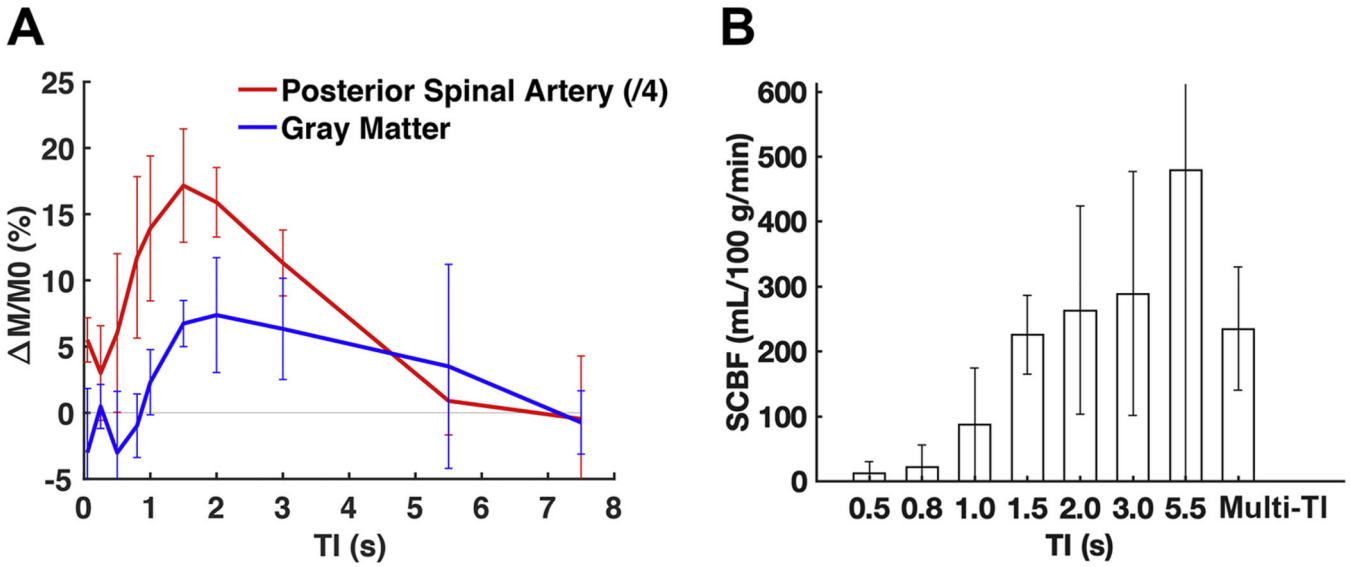

Figure 3.

Perfusion weighted contrast and SCBF changes across different inversion times (TI). (A) Perfusion weighted contrast (ΔM/M0) as a function of inversion time for the posterior spinal arteries (red; scaled by 1/4) and gray matter (blue) in sham animals (n=6). A short transit time delay effect is somewhat evident in the artery, and the contrast in the gray matter lags the arterial changes, as expected. (B) In gray matter ROIs in sham animals, the SCBF estimates for single-TI delays plateaus at 1.5 s, with values consistent with the multi-TI SCBF using all TI times. The inter-animal variability is also lowest at the 1.5 s TI. Error bars mean the standard deviations in both figures.

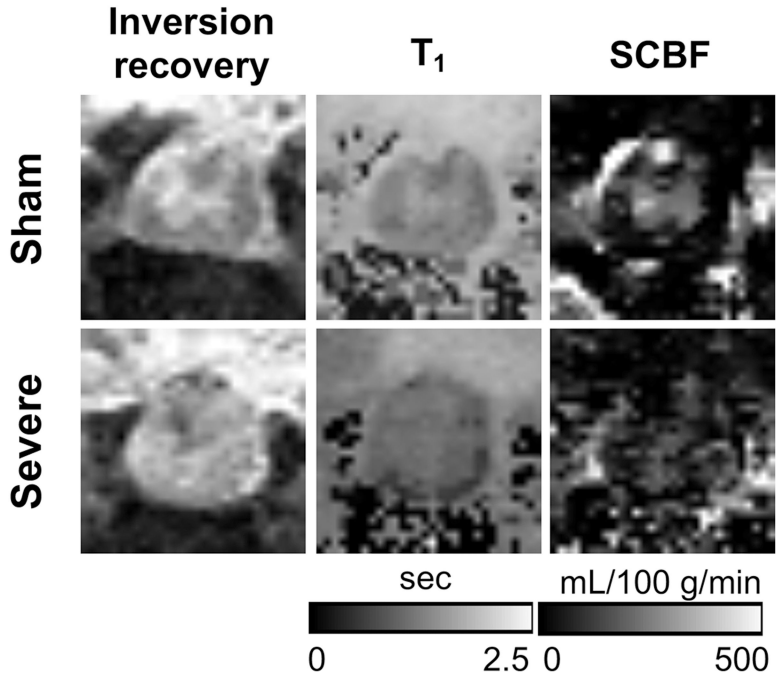

Figure 4.

Representative inversion recovery images (TI=5000 ms), quantitative T_1, and SCBF maps. The loss of gray and white matter contrast in the injured animal is evident.

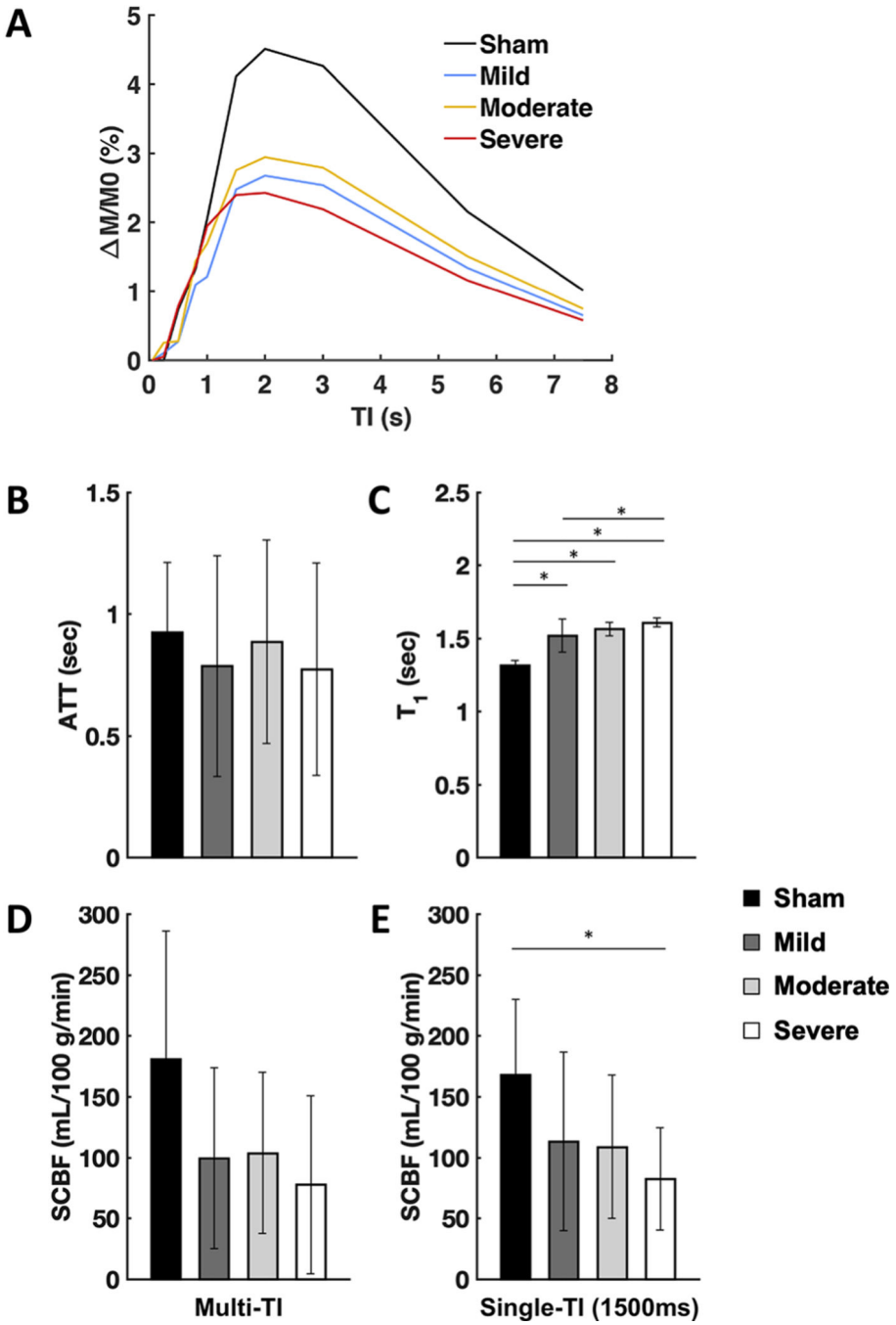

Figure 5.

Summary of metrics derived by FAIR. (A) Mean perfusion weighted contrast (DM/M0) as a function of inversion time for the whole-cord ROIs at the injury epicenter grouped by injury severity. For better visualization, estimates of group variability are not shown. (B) Arterial transit time (ATT) did not differ by severity. (C) T_1 relaxation time constant increased as severity increased. (D) Multi-TI SCBF estimates were decreased after injury, but no consistent relationship of severity was evident.(E) Single-TI estimates of SCBF (TI=1500 ms) exhibited a similar trend but with severe injury having a significant decrease compared

to sham animals. Error bars indicate standard deviation. *-significant difference at $p < 0.05$ (2-tailed).

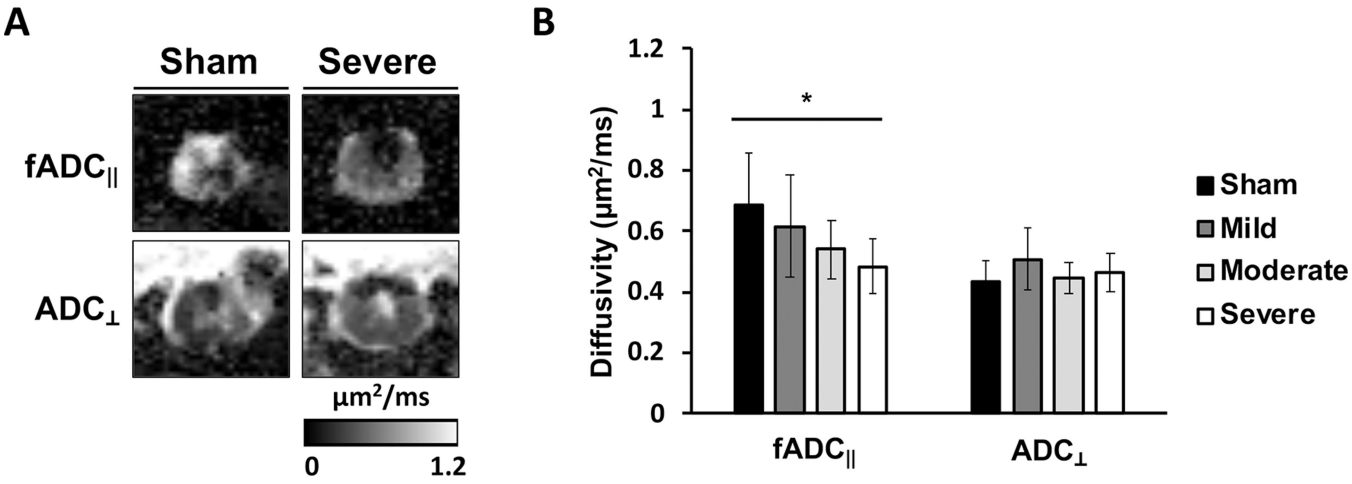

Figure 6.

Diffusion MRI at the lesion site. (A) Representative $fADC_{\parallel}$ and $ADC_{\perp}$ in the sham and severe animals. (B) The decreasing trend of $fADC_{\parallel}$ was observed with increasing severity. Error bars indicate standard deviation. *-significant difference at $p< 0.05$ (2-tailed).

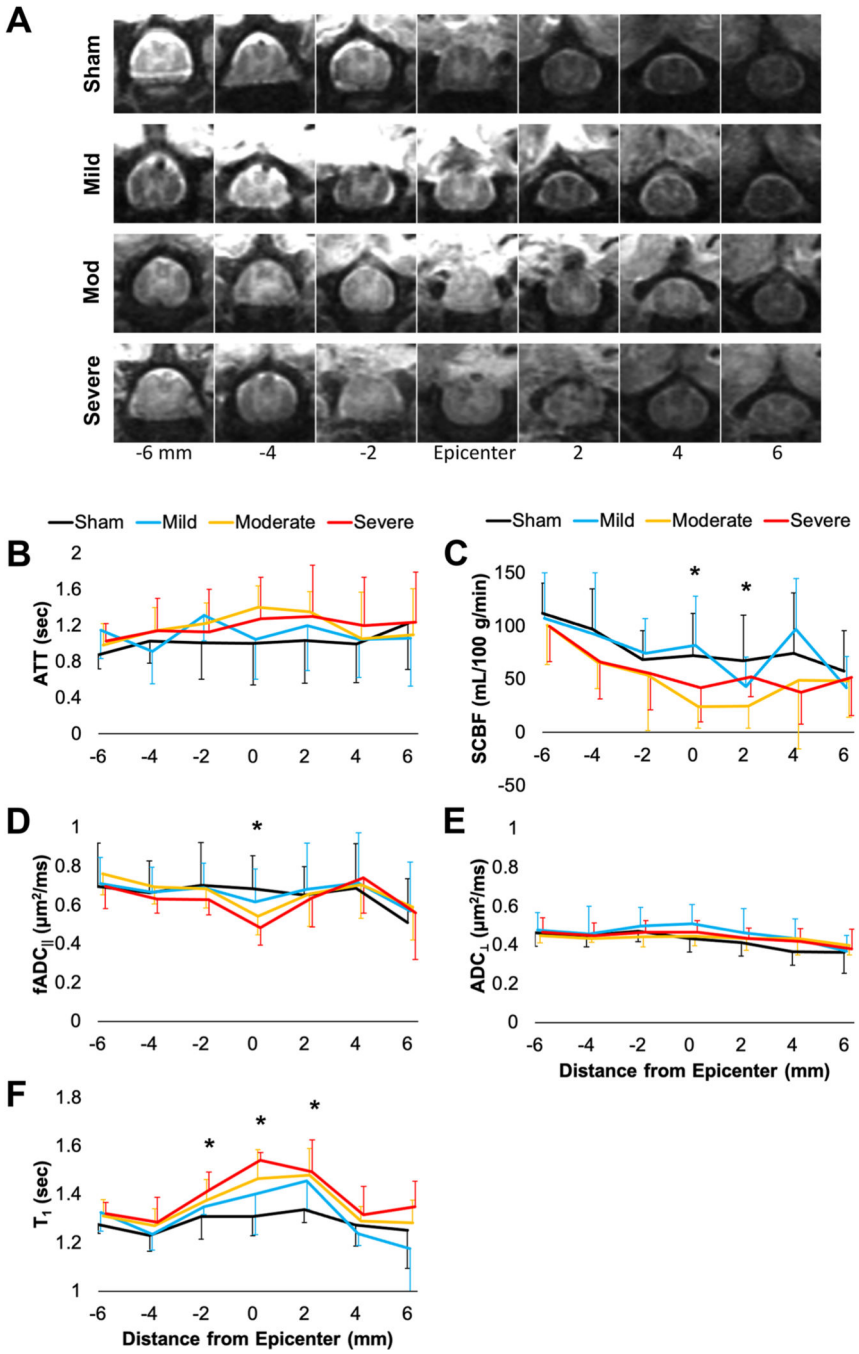

Figure 7.

Summary of whole-cord ROI mean values across the lesion site. Representative images (TI=7500 ms) from each injury severity (A). ATT (B) from multi-TI analysis did not appreciably differ across the cord or between different severities. SCBF (C) from single-TI (1500 ms) was significantly related to severity at the site of injury and one slice above the lesion. $fADC_{\parallel}$ (D) was significantly related to severity at the lesion site but did not differ above or below the lesion. $ADC_{\perp}$ (E) was not changed with injury. T_1 (F) was significantly related to severity at the lesion site and one slice above and below. For better visualization,

only positive or negative error bars are shown and indicate standard deviation. *-Main effect of injury severity, $p<0.05$.

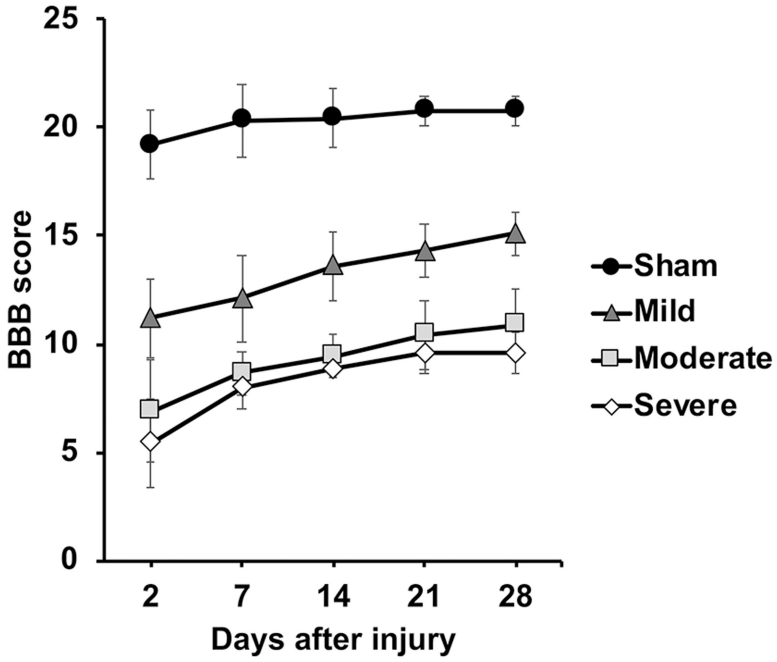

Figure 8.
Neurobehavioral scores obtained weekly. Error bars indicate standard deviation.

Table 1.

Correlation of MR metrics with BBB score at 28 days

		Sham included (n=33)		Sham excluded (n=25)	
Method	**Metrics**	**R^2**	**p value**	**R^2**	**p value**
FAIR	SCBF	0.233**	0.004	0.063	0.228
	T_1	0.709**	<0.001	0.432**	<0.001
DWI	$fADC_{\parallel}$	0.270**	0.002	0.232*	0.015
	$ADC_{\perp}$	0.004	0.742	0.193*	0.028

Note: SCBF=Spinal cord blood flow; T_1=T_1-relaxation time; $fADC_{\parallel}$=Filtered axial diffusivity; $ADC_{\perp}$=Perpendicular diffusivity

*correlation is significant at the 0.05 level (2-tailed)

**and at the 0.01 level (2-tailed).